agriculture

MDPI

Article

Dynamics of Microbial Community Structure and Metabolites during Mulberry Ripening

Minghong Bian †, Yuli Fang †, Tianmeng Yuan, Qiang Xu, Yubin Xia, Hongyi Tang, Yiling Feng and Baolin Han *

College of Biological Engineering, Sichuan University of Science & Engineering, 188 University Town, Yibin 644000, China; bmhsuse@suse.edu.cn (M.B.); 322086002322@stu.suse.edu.cn (Y.F.); 321086002231@stu.suse.edu.cn (T.Y.); 20041060317@stu.suse.edu.cn (Q.X.); 22041060315@stu.suse.edu.cn (Y.X.); 21041050122@stu.suse.edu.cn (H.T.); 22041060324@stu.suse.edu.cn (Y.F.)

* Correspondence: han_bl1986@suse.edu.cn; Tel.: +86-178-2810-8622

† These authors contributed equally to this work.

Abstract: In this experiment, we explored the chemical composition and community structure of Mulberry "Wuhedashi" (*Morus alba* L., hereinafter referred to as WHDS) in different stages and obtained data support for its resource utilisation. Five ripening stages were established: S1, deep-red stage; S2, red with black stage; S3, black with red stage; S4, black stage; S5, overripe stage. The results showed that there were significant differences in the indicators of WHDS in the different stages. Immature WHDS contains high levels of amino acids (2.14 ± 0.15 mg/g), organic acids (43.10 ± 0.75 mg/g), K (3019.52 ± 78.00 mg/L), and Ca (1617.86 ± 24.45 mg/L) and is an important source of amino acid and mineral supplementation for the body. Total phenolic compounds (26.15 ± 0.43 g/L), total flavonoids (2.46 ± 0.03 g/L), total anthocyanins (587.60 ± 7.38 mg/L), the ABTS radical scavenging rate (94.20 ± 2.18%), the DPPH radical scavenging rate (95.13 ± 1.44%), and total flavour compounds (1279.09 ± 33.50 mg/L) peaked at S4, which is the optimal stage for the consumption and processing of WHDS. High-throughput sequencing identified 10 dominant genera, including *Bacillus*, *Brevibacterium*, *Pseudomonas*, and *Tatumella*. *Nesterenkonia* was the most highly associated micro-organism. Bacterial genera such as *Pantoea* and *Pseudomonas* were significantly positively correlated with esters, enhancing the floral and fruity flavours of wine. The results of the study revealed the characteristics of WHDS in different stages, which can help to target the development of nutritious mulberry derivatives and provide a reference for enhancing the added value of mulberry.

Keywords: mulberry; minerals; microbial community; volatile flavour compounds; correlation analysis

check for updates

Citation: Bian, M.; Fang, Y.; Yuan, T.; Xu, Q.; Xia, Y.; Tang, H.; Feng, Y.; Han, B. Dynamics of Microbial Community Structure and Metabolites during Mulberry Ripening. *Agriculture* **2024**, *14*, 1129. https://doi.org/10.3390/agriculture14071129

Academic Editor: Isabel Lara

Received: 11 June 2024
Revised: 2 July 2024
Accepted: 10 July 2024
Published: 12 July 2024

Copyright: © 2024 by the authors. Licensee MDPI, Basel, Switzerland. This article is an open access article distributed under the terms and conditions of the Creative Commons Attribution (CC BY) license (https://creativecommons.org/licenses/by/4.0/).

1. Introduction

Mulberry, also known as mulberry fruit, mulberry seed, and mulberry jujube, is a kind of juicy berry obtained from the mulberry tree with a long history of cultivation, mainly grown in Sichuan and Hunan provinces [1]. Since ancient times, mulberry has enjoyed the reputation of the "fruit king;" its soft and juicy flesh is not only rich in a variety of nutrients but also known to lower blood glucose and cholesterol and reduce symptoms of arthritis [2] and so can be used as both medicine and food [3]. The carbohydrates [4], amino acids [5], vitamins, and minerals [6], such as Se, Ca, and Fe, contained in mulberries are important nutrients required by the human body. Existing studies have shown that mulberries can regulate the body's immune function, promote the growth of haematopoietic cells, and have health effects such as anti-mutagenesis and the lowering of blood lipids [7]. Although the nutritional value of fresh mulberries is extremely high, their shelf life is only 1–2 days [8], and they are prone to decay and deterioration during transport and sale. In order to maximise the retention of the nutrients of the mulberry, increase the added value of its

products, and meet consumer requirements, it is particularly important to choose the best picking stage.

Mulberry is popular not only for its rich nutritional value and health benefits but also for its unique sweet and sour flavour [9]. During the ripening stage, the colour of the skin will gradually change from an initial greenish colour to deep red, then to deep purple and, finally, to completely black; meanwhile, the taste changes from an initial hard astringency to a delicate and soft flavour. Amino acids [10], organic acids [11], and sugars—as precursors of flavour substances—produce dozens of volatile flavour substances, such as esters, alcohols, and terpenes, after complex chemical reactions [12], which give mulberries their strong floral, nutty, and fruity aromas [13]. Therefore, an in-depth study of the unique substance composition of mulberry at different stages of ripening is of great significance for understanding the mechanism of mulberry flavour formation and enhancing its quality.

To date, studies on the quality characteristics of mulberries at different maturity levels have mainly focused on their physicochemical properties and mineral content. Lin et al. [14] found that ripe mulberries contain high levels of total sugars and total phenols, at 129.88 ± 1.09 mg/g and 3.08 ± 0.16 mg/g, respectively, which make them a good choice as a dietary supplement. Comparatively, unripe mulberries contain high mineral and organic acid contents, which allows them to be used as food additives or stabilisers. A study by Hu et al. [15] indicated that the flavonoid content of mulberry increases after ripening. However, there are relationships among the quality indicators of mulberry, which may lead to an overlap of the many pieces of information reflected by the indicators, and systematic evaluation eliminates these overlapping pieces of information. Currently, there are relatively few comprehensive studies on key characteristics such as antioxidant capacity, flavour substances, and microbial community succession in mulberries at different maturity levels.

In this study, high-throughput sequencing was used to analyse and characterise the composition and succession of the microbial community during mulberry ripening. Meanwhile, headspace solid-phase microextraction–gas chromatography–mass spectrometry (HS-SPME-GC-MS) was used for a detailed analysis of the volatile flavour substances in mulberries. In addition, we examined the contents of non-volatile metabolites and minerals during the ripening process. The aim was to study the evolution of basic physicochemical indices, metabolite changes, and microbial community structure during the ripening process of Nucellar Big Ten and to explore the correlation between key flora and physicochemical properties and flavour substance species. The results of this study provide a reference for a further in-depth understanding of the quality characteristics of mulberry and allow for a scientific and reasonable determination of its harvesting time.

2. Materials and Methods

2.1. Fruit Materials

WHDS was harvested from a mulberry orchard in Changning County, Yibin City, Sichuan Province, China. The geographical coordinates are roughly located in the area from 104°44′22″ to 105°03′30″ east longitude and 28°15′18″ to 28°47′48″ north latitude, with a humid subtropical monsoon climate. Every year in April, the area welcomes the mulberry harvest season. The soil in this region is mainly loess and purple soil with a pH between 5 and 7, rich and balanced in nutrients. The morphological characteristics of S1, S2, S3, S4, and S5 are shown in Figure 1. A random sampling method was used, where 20–50 mulberry trees were randomly selected from the orchard, and 10–20 mulberry fruits were picked from each tree. Mulberries that were not damaged or spoiled were selected for the experiment, followed by immediate freezing in liquid nitrogen and storage at −80 °C to facilitate the next step of random-sample analysis (n = 3).

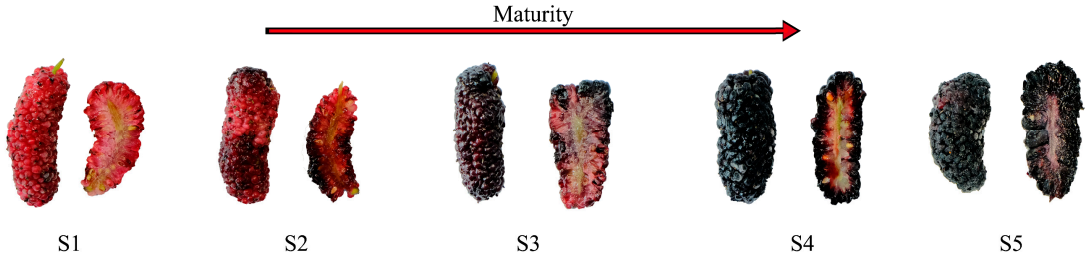


Figure 1. WHDS at different maturity stages. **Note:** S1, the fruits are reddish in colour, small in size, astringent, hard, and nutritious but less ripe for consumption. S2, mulberries gradually change from red to black, the taste begins to become sweet but is still slightly astringent, and the flesh is firmer; they can be eaten in moderation. S3, mulberries ripen further and turn black in colour. Mulberries at this stage taste sweet and moist, the astringency is basically gone, and the flesh is softer and more palatable. S4, mulberries are fully ripe, turning black in colour, are very sweet in taste, with soft and juicy flesh, and are very tasty; this stage is the best time to eat them. S5, mulberries continue to ripen, turning purplish black in colour, and are still sweet and moist in taste, but the flesh is beginning to soften.

2.2. Raw Materials and Reagents

The standards for the quantitative analysis of amino acids (HPLC, purity $\geq$ 98), organic acids (HPLC, purity $\geq$ 98), and volatile compounds (GC, purity $\geq$ 98) in the experiments were purchased from Sigma-Aldrich Corporation, St. Louis, MO, USA. The other analytical-grade chemicals were supplied by the Chemical Reagent Factory (Chengdu, China).

2.3. Measurement of Basic Physiological Indicators

2.3.1. Fruit Weight, Total Soluble Solids, Juice Yield, and pH Value

The pH values were determined using a pH meter (PHS-3C, Shanghai, China). Individual fruit weights were determined using an electronic balance (HX3002T, Zhejiang, China). Soluble solids were determined using a portable digital saccharimeter (HSU-20, Shanghai, China). Approximately 10 g of mulberry pulp was weighed and recorded as mass m_1. The pulp was ground and centrifuged in a centrifuge tube at 12,000 g for 10 min, the supernatant was discarded, and the mass of the residue was recorded as m_2. The juice yield was calculated using Equation (1):

$$X = \frac{m_1 - m_2}{m_1} \times 100\% \quad (1)$$

where X denotes the mulberry juice yield (%); m_1 denotes the mass of the weighed mulberry (g); and m_2 denotes the mass of the residue (g).

2.3.2. Total Acid

The total acid was determined according to the GB/T 15038-2006 "General Methods of Analysis for Wines and Fruit Wines" methods [16]. The steps are as follows: place 10 mL of mulberry juice into a 100 mL beaker, calibrate the automatic spot titrator (ZDJ-3A, Shanghai, China) with pH 8.0 buffer solution, immerse the electrode in the mulberry juice, and titrate the solution with sodium hydroxide (0.1 mol/L) to pH 8.2. The total acid was calculated using Equation (2):

$$X = \frac{c \times (V_1 - V_0) \times 75}{V_2} \quad (2)$$

where X denotes the total acid content (g/L); c denotes the concentration of the sodium hydroxide standard titration solution (mol/L); V_1 and V_0 denote the volumes of the sodium hydroxide standard titration solution consumed for the titration and blank tests, respectively (mL); V_2 denotes the volume of the sample (mL); and 75 denotes the value of the molar mass of tartaric acid (g/mol).

2.3.3. Total Sugars

The total sugars were determined using the method of Liu et al. [17] with minor modifications. The steps are as follows: Pipette 0.5 mL of mulberry juice into a 2.0 mL centrifuge tube with a pipette gun, add 220–300 µL of 3,5-dinitrosalicylic acid (DNS, 6.3 g/L) solution, and mix well. Continue to add ultrapure water to 2.0 mL, place the sample in a water bath at 60–100 °C for 3–7 min to develop the colour, remove, and immediately cool rapidly to room temperature in an ice water bath. The absorbance values were determined at 510 nm after shaking well, and, finally, the total sugar content was calculated using a glucose standard curve.

2.3.4. Determining the Content of Phenolic Compounds

The determination of phenolics was based on the method described by Xia et al. [18] with minor modifications. In brief, 0.2 g of mulberry sample was ground into a homogenate with cold 70% (*v*/*v*) methanol containing 2% (*v*/*v*) formic acid and 28% (*v*/*v*) ethanol. The homogenate was sonicated for 30 min, followed by shaking at 30 °C for 2 h at 300 rpm. Then, the homogenate was centrifuged at 10,000 g for 10 min at 4 °C, and the supernatant was filtered through a 0.45 µm membrane for further analysis.

The total phenol content was determined using the Folin–Ciocalteu method; the absorbance was measured at 765 nm, and the results are expressed as gallic acid equivalents. The absorbance of total flavonoids was measured at 510 nm and is expressed as rutin equivalents. The anthocyanin content was determined using the pH-differential method, in which mulberry extracts were diluted 10-fold with buffer solutions of pH 1.0 and 4.5; the absorbance values at each pH were measured at 519 nm and 700 nm, and then the anthocyanin content was calculated as the difference between the two.

2.4. Determination of Antioxidant Capacity

2.4.1. Determination of ABTS Radical Scavenging Activity (Hereinafter Referred to as ABTS RSA)

The method described by Wang et al. [19] was used with minor modifications. The steps are as follows: Take 0.1 g of mulberry sample and add 0.9 mL of water and 3 mL of ABTS solution. Mix and shake well, react for 6 min away from light, and then measure the absorbance at 734 nm. In our test, 0.1 g of mulberry sample with 3.9 mL of distilled water was used as a blank group. Meanwhile, 1 mL of distilled water with 3 mL of ABTS solution was used for the blank control group absorbance. The ABTS RSA was calculated using Equation (3):

$$\text{ABTS RSA} = (1 - \frac{A_1 - A_0}{A_2}) \times 100\% \quad (3)$$

where A_1 is the absorbance of the sample, A_0 is the absorbance of the blank, and A_2 is the absorbance of the control.

2.4.2. Determination of DPPH Radical Scavenging Activity (Hereinafter Referred to as DPPH RSA)

The method described by Zhou et al. [20] was used with minor modifications. The fermentation broth was diluted 5 times as the sample solution, and 1.0 mL of the fermentation broth was added to 3.0 mL of DPPH solution (0.1 mmoL/L), mixed well, and then reacted for 30 min at room temperature and protected from light. The absorbance of the sample was measured at 517 nm, and vitamin C (0.03 mg/mL) was used as the control solution. The DPPH RSA was calculated using Equation (4):

$$\text{DPPH RSA} = (1 - \frac{A_1 - A_0}{A_2}) \times 100\% \quad (4)$$

where A_1 is the absorbance of the sample, A_0 is the absorbance of the blank, and A_2 is the absorbance of the control.

2.5. Determination of Organic Acids

The organic acid content was determined according to the method reported by Scutarașu et al. [21], but with minor adjustments to the mobile phase and elution procedure. An HPLC system (Agilent, Santa Clara, CA, USA) equipped with a ZORBAX SB-Aq column (4.6 × 250 mm, 5 µm, Thermo Fisher Scientific, Waltham, MA, USA) was used according to a previous method. The mobile phase consisted of a KH_2PO_4 solution (pH 2.3, 0.01 mol/L), and the organic acids were separated using a 100% mobile phase elution procedure. Other parameters were as follows: the flow rate was 1 mL/min, the column temperature was 25 ± 0.5 °C, the detection wavelength was 210 nm, the injection volume was 20 µL, and the total run time was 20 min. Table S1 of the Supplementary Material demonstrates the quantitative parameters of the organic acid standards.

2.6. Determination of Amino Acids

The amino acids were determined according to the method reported by Xu et al. [22] with slight modifications. After centrifugation, 1 mL of the sample supernatant and 1 mL of the standard solution were placed in a 15 mL centrifuge tube, and 500 µL of acetonitrile solution of phenyl isothiocyanate (0.2 mol/L) and 500 µL of acetonitrile solution of triethylamine were added (1 mol/L). The reaction was terminated by adding 100 µL of acetic acid with a mass fraction of 20% at room temperature for 1 h. Later, 2 mL of n-hexane (AR) was added to the above reaction solution after derivatisation and mixed well by shaking for 60 s. Then, the solution was allowed to stratify, and the upper layer of the solution was discarded. The lower layer of the solution was sucked up using a sterile syringe, transferred to a liquid-phase bottle after filtration with a 0.22 µm organic filtration membrane, and kept at −20 °C for spare use.

Mobile phase A was prepared as follows: 0.02 mol/L of anhydrous sodium acetate solution was added to 0.5 mL of triethylamine and fixed to 1000 mL with deionised water at pH 8.2. Mobile phase B was prepared as follows: acetonitrile–water = 80:20, v:v. Other parameters were as follows: a flow rate of 1.0 mL/min, column temperature of 40 ± 0.5 °C, detection wavelength of 254 nm, and injection volume of 10 µL. Table S2 of the Supplementary Material demonstrates the quantitative parameters of the amino acid standards.

2.7. Determination of Mineral Content

The mineral content was determined according to the method reported by Shimizu et al. [23]. Here, 1 g of sample was weighed and placed into the dissolution tube, 5 mL of nitric acid solution (65%, AR) and 1 mL of hydrogen peroxide (30%, AR) were added, the cap was tightened, and the sample was shaken slowly. The sample was then placed in a microwave dissolution oven and dissolved until the solution became transparent. The ablation tube was then placed on an electric heater at 180 °C to drain the acid, and, when the liquid in the tube was approximately 1 mL, the remaining liquid was transferred to a 25 mL test tube with ultrapure water. The above solutions were appropriately diluted and detected using ICP-MS (7770x, Agilent Technologies, CA, USA). The concentrations of the four minerals (K, Ca, Fe, and Se) were quantified via the external standard method, and the concentration ranges of the standard solutions were set to 0, 1, 5, 10, 50, 100, 500, 1000, and 5000 µg/L.

2.8. Analysis of Volatile Compounds

The volatile compounds were determined according to the method reported by Ji et al. [24], but with slight modifications. The procedure was as follows: Firstly, 5.0 g of mulberry was ground into a homogeneous pulp and transferred to a 15 mL headspace flask. Then, 1.0 g of NaCl and 40 µL of the internal standard substance (ethyl valerate at a concentration of 1 mg/mL) were added. The sample was equilibrated at 60 °C for 15 min to allow sufficient time for the volatile compounds to enter the gas phase in the headspace vial. Next, volatile compounds were adsorbed using a solid-phase microextraction (SPME) fibre coated

with 50/30 µm divinylbenzene/carboxylate/polydimethylsiloxane (DVB/CAR/PDMS) for 30 min at 45 °C. Afterwards, the SPME fibres were placed into a GC-MS system (6890N/5975B, Agilent Technologies Co., Ltd.; Santa Clara, CA, USA) and desorbed at 250 °C for 5 min. The other test parameters were as follows: Helium with a purity higher than 99.999% was used as the carrier gas, and the flow rate was set to 1 mL/min. The temperature of the inlet port was set to 270 °C, and a non-split injection was used. In addition, an EI ionisation source (70 eV) was used with an ion source temperature of 230 °C and an interface temperature of 280 °C. The full scan range was m/z 35–550. The detected volatiles' mass spectra were compared and matched with the NIST17.L standard mass spectrograms to qualitatively analyse the detected compounds. Figure S1 of the Supplementary Material illustrates the chromatogram of the internal standard for volatile flavour substances.

2.9. Metagenomic DNA Extraction, Amplification, and Sequencing

DNA extraction was performed using the standard procedure of the Fast DNA SPIN Kit (MP Biomedicals, Irvine, CA, USA), and the purity, concentration, and integrity of the DNA were assessed using agarose gel electrophoresis to ensure that high-quality DNA was obtained that was suitable for the study. The primers 799F (5′-AACMGGATTAGATACCCKG-3′) and 1193R (5′-ACGTCATCCCCACCTTCC-3′) were used to amplify 16sRNA from the bacterial V3–V4 region. The amplification system included 4 µL of 5 × Fast Pfu buffer, 2 µL of 2.5 mM dNTPs, 0.8 µL of each primer (5 µM), 0.4 µL of Fast Pfu polymerase, 10 ng of template DNA, 0.2 µL of BSA, and ddH_2O to reach a final volume of 20 µL. The PCR amplification cycling conditions were as follows: initial denaturation at 95 °C for 3 min; denaturation at 95 °C for 30 s; annealing at 55 °C for 30 s; 72 °C extension for 45 s and 27 cycles (bacteria); and complementary extension at 72 °C for the last 10 min. Each sample was subjected to three PCR cycles and mixed. The PCR products were detected using 2% agarose gel electrophoresis, and the PCR products were initially quantified according to the electrophoresis results. The PCR products were then sent to Shanghai Majorbio Bio-Pharm Technology Co., Ltd. for sequencing for subsequent analysis.

2.10. Statistical Analyses

All data are expressed as the mean ± SD of three independent experiments (n = 3). Differences among different groups were evaluated through one-way analysis of variance (ANOVA) using SPSS 18.0 software (SPSS Inc., Chicago, IL, USA). A value of $p < 0.05$ was considered statistically significant. Line charts, heat maps, Veen charts, etc., were plotted using the Origin 2022 (Origin Lab, Northampton, MA, USA) software. Principal component analysis (PCA) was performed using SIMCA 14.1 (Umetrics AB, Umea, Vasterbotten, Sweden). Based on Spearman's correlation coefficients, potential correlations between physicochemical properties and metabolites with major microbial taxa were calculated using R software and Gephi (v0.9.5).

3. Results and Discussion

3.1. Dynamic Changes in Basic Physiological Indicators of WHDS during Ripening

The physicochemical differences in WHSD at different ripening stages were significant and were analysed by measuring the pH, weight of single fruit, soluble solids, juice yield, total acid, and total sugar. As can be seen in Table 1, the pH of the seedless Big Ten ranged from 3.55 ± 0.02 to 3.78 ± 0.04; the weight of the individual fruits increased with maturity and reached a maximum value of 2.08 ± 0.02 g at S4. WHSD belongs to the aggregation class of drupes, where the level of juice yield affects the flavour and texture of the fruit, as well as fruit wine fermentation production. It had a juice yield above 20% throughout the ripening stage, which increased significantly ($p < 0.05$) from 23.05 ± 0.29% in S1 to 52.76 ± 0.38% in S4. Both soluble solids and total sugars in WHDS increased significantly ($p < 0.05$) with maturity from 8.85 ± 0.41 B.rix to 21.64 ± 0.58 B.rix and 0.22 ± 0.02 g/L to 0.92 ± 0.66 g/L, respectively, whereas the total acid content decreased significantly ($p < 0.05$) with maturity, which is highly similar to that of grape ripening [25].

Table 1. Dynamic changes in basic physiological indicators of WHDS during ripening.

Phase	S1	S2	S3	S4	S5
pH	3.55 ± 0.02^{c}	3.46 ± 0.03^{d}	3.78 ± 0.04^{a}	3.66 ± 0.04^{b}	3.68 ± 0.03^{b}
Weight of single fruit (g)	1.47 ± 0.01^{d}	1.60 ± 0.01^{c}	1.98 ± 0.02^{b}	2.08 ± 0.02^{a}	2.07 ± 0.03^{a}
Soluble solids (B.rix)	8.85 ± 0.41^{e}	10.08 ± 0.25^{d}	11.25 ± 0.33^{c}	18.94 ± 0.22^{b}	21.64 ± 0.58^{a}
Juice yield (%)	23.05 ± 0.29^{e}	32.10 ± 0.09^{d}	43.71 ± 0.70^{c}	52.76 ± 0.38^{a}	51.67 ± 0.36^{b}
Total acid (g/L)	5.39 ± 0.02^{a}	3.75 ± 0.03^{b}	2.64 ± 0.02^{c}	1.55 ± 0.03^{d}	0.39 ± 0.03^{e}
Total sugar (g/L)	0.22 ± 0.02^{e}	0.31 ± 0.06^{d}	0.58 ± 0.04^{c}	0.71 ± 0.14^{b}	0.92 ± 0.66^{a}
Total phenolics (g/L)	7.13 ± 0.03^{e}	10.06 ± 0.20^{d}	11.47 ± 0.11^{c}	26.15 ± 0.43^{a}	17.35 ± 0.18^{b}
Total flavonoids (g/L)	0.89 ± 0.01^{c}	1.65 ± 0.02^{b}	1.38 ± 0.01^{b}	2.46 ± 0.03^{a}	1.78 ± 0.04^{b}
Total anthocyanins (mg/L)	74.73 ± 0.62^{e}	110.74 ± 1.54^{d}	185.97 ± 2.72^{c}	587.60 ± 7.38^{a}	341.09 ± 4.81^{b}

Note: Different lowercase letters represent significant differences in factors at $p < 0.05$.

Existing research shows that mulberry is rich in phenols, flavonoids, anthocyanosides, and other biologically active substances; the appropriate consumption of polyphenolic fruits can reduce the incidence of cardiovascular disease, liver disease, and other diseases while also slowing down the oxidation of cells, thus playing an anti-ageing role [26,27]. As shown in Table 1, the total phenol content of WHDS ranged from 7.13 ± 0.03 g/L to 26.15 ± 0.43 g/L, and the total flavonoids ranged from 0.89 ± 0.01 g/L to 0.89 ± 0.01 g/L, both of which increased with maturity and both of which peaked at S4. Anthocyanins enriched in mulberries are natural colouring agents [28], with the six most common being geranium, cornflower, delphinium, peony, petunia, and mallow pigments [29]. Glycosylated and acylated anthocyanins have strong stability [30], so the anthocyanins found in the fruits are mainly present in the form of anthocyanosides after harvesting. The anthocyanins in WHDS increased significantly from 72.73 ± 0.62 mg/L in S1 to 587.60 ± 7.38 mg/L in S4 ($p < 0.05$) and then decreased significantly to 341.09 ± 4.81 mg in S5 ($p < 0.05$). The anthocyanin content in S4 was about 3–10 times higher than that of grapes [31], making this the best time to obtain the natural pigments and supplement with anthocyanin.

3.2. Dynamic Changes in Antioxidant Capacity of WHDS during Ripening

According to the doctrine of oxygen radicals, biological oxidation can be harmful to human health and cause diseases [32], and the antioxidant substances in fruits can scavenge a certain amount of reactive oxygen species (ROS) to keep them in a dynamic equilibrium [33] and protect the body from oxidative damage. The antioxidant capacity of fruits is usually represented by indicators such as ABTS RSA and DPPH RSA [34], with higher scavenging rates corresponding to higher antioxidant capacity. WHDS samples at different maturity levels had some differences in their final antioxidant capacity due to differences in phenolics and flavonoids. As shown in Figure 2a, the ABTS RSA of WHDS was in the range of 0%–94.20 ± 2.18%, with the peak occurring at S4. For the same maturity and at different concentrations, the ABTS RSA increased with maturity, with clearance basically stabilising at around 91% at S4. For different maturities and at the same concentration, ABTS RSA did not behave in a regular manner, with low clearance at a sample volume of 0.02 mL and three stages below 50%. As shown in Figure 2b, the trends in DPPH RSA were similar to those in ABTS RSA, which coincided with the trend in grapevine growth [35], with total clearance ranging from 0% to 95.13 ± 1.44%, with the peak occurring at S4 and slightly higher than that of ABTS RSA. Clearance was also relatively low at a sample volume of 0.02 mL, with three stages below 50%, until it essentially stabilised at 0.08 mL at approximately 91%. Notably, the antioxidant capacity of WHDS increased with maturity, which is highly similar to the trend in the antioxidant capacity of plums [36], and most of their peaks occurred at S4, suggesting that this may be the optimal consumption stage for the human body to improve antioxidant capacity and scavenge free radicals.

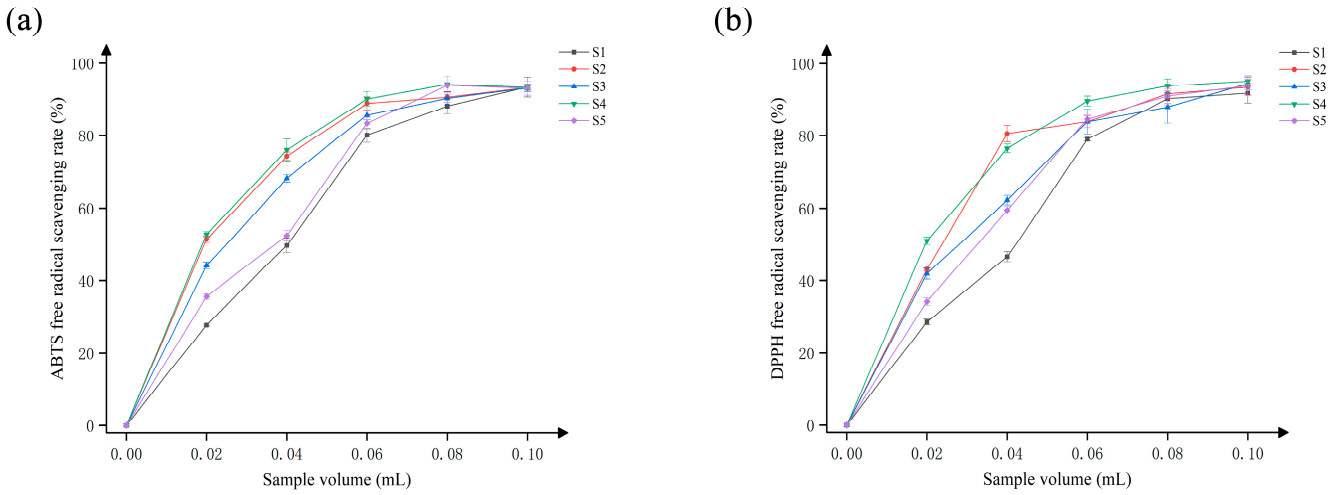


Figure 2. Alterations in ABTS RSA (**a**) and DPPH RSA (**b**) at different maturity stages of WHDS.

3.3. Dynamic Changes in Organic Acids in WHDS during Ripening

Organic acids are important components in determining the acidity of mulberry fruit, and their content and type have a direct impact on the flavour and texture of mulberries. A total of 10 organic acids—tartaric acid, pyruvate, malic acid, lactic acid, fumaric acid, citric acid, succinic acid, oxalic acid, acetic acid, and α-ketoglutaric acids—were tested to determine the changes in WHDS during maturation using high-performance liquid chromatography (HPLC), and the results are shown in Table 2. Tartaric acid is an important organic acid found in mulberry fruits and is also the most abundant organic acid in WHDS, which not only has strong chemical stability but also exhibits certain antibacterial properties [37]. The tartaric acid content of WHDS showed a decreasing trend with the increase in maturity and was highest in S2 at 16.45 ± 0.24 mg/L and lowest in S5 at 9.24 ± 0.14 mg/L. Lactic acid and acetic acid were placed second and third in organic acid content, and both reached their maximum values at S2 with 10.34 ± 0.13 mg/L and 9.94 ± 0.16 mg/L, respectively. Lactic and acetic acids are common organic acids found in fruits, and applying acetic acid to the skin of growing fruits also improves post-harvest fruit quality [38]. Malic acid and fumaric acid are the main organic acids in mulberry, with maximum contents of 2.73 ± 0.04 mg/L and 1.34 ± 0.12 mg/L, respectively, and the total of the two accounts for about 10% of the organic acids. Oxalic acid levels ranged from 0.50 ± 0.10 mg/L to 0.95 ± 0.02 mg/L with little overall variation. α-Ketoglutaric acid, citric acid, and pyruvic acid are the main contributors to the acidity of the fruit [39,40], and their levels during ripening in WHDS did not differ much, with maxima of 0.47 ± 0.01 mg/L, 0.47 ± 0.01 mg/L, and 0.43 ± 0.02 mg/L, respectively, whereas succinic acid was only detected in S1, at 0.11 ± 0.01 mg/L.

It is worth noting that, except for succinic acid and citric acid, the trends in the contents of the other eight organic acids increased and then decreased, with the peaks occurring at S2, which is basically consistent with the results of a study on the ripening stage of plum fruits [41]. It can be seen that there are large differences in the composition of organic acids at different maturity stages of WHDS, and the adulteration of WHDS with different maturity levels in the same production process may lead to an imbalance in the flavour of fruit wines, fruit vinegars, and other beverages, affecting the quality of the products.

Table 2. Dynamic changes in organic acid contents in WHDS during ripening.

Phase	S1	S2	S3	S4	S5
Tartaric acid (mg/g)	12.55 ± 0.23^{b}	16.45 ± 0.24^{a}	11.24 ± 0.07^{c}	9.64 ± 0.08^{d}	9.24 ± 0.14^{e}
Lactic acid (mg/g)	8.95 ± 0.05^{b}	10.34 ± 0.13^{a}	7.73 ± 0.06^{c}	6.53 ± 0.18^{d}	6.15 ± 0.22^{e}
Acetic acid (mg/g)	7.84 ± 0.24^{b}	9.94 ± 0.16^{a}	6.64 ± 0.14^{c}	5.83 ± 0.19^{d}	5.62 ± 0.12^{d}
Malic acid (mg/g)	2.14 ± 0.17^{b}	2.73 ± 0.04^{a}	1.96 ± 0.21^{b}	1.63 ± 0.11^{c}	1.72 ± 0.10^{c}
Fumaric acid (mg/g)	1.27 ± 0.18^{a}	1.34 ± 0.12^{a}	1.30 ± 0.01^{a}	0.89 ± 0.03^{b}	0.94 ± 0.11^{b}
Oxalic acid (mg/g)	0.74 ± 0.22^{ab}	0.95 ± 0.02^{a}	0.60 ± 0.07^{b}	0.55 ± 0.19^{b}	0.50 ± 0.10^{b}
α-Ketoglutaric acids (mg/g)	0.35 ± 0.17^{a}	0.47 ± 0.01^{a}	0.35 ± 0.18^{a}	0.23 ± 0.11^{a}	0.23 ± 0.07^{a}
Citric acid (mg/g)	0.47 ± 0.01^{a}	0.45 ± 0.01^{a}	0.34 ± 0.11^{b}	0.29 ± 0.01^{b}	0.33 ± 0.04^{b}
Pyruvate (mg/g)	0.33 ± 0.05^{ab}	0.43 ± 0.02^{a}	0.35 ± 0.11^{ab}	0.23 ± 0.07^{b}	0.23 ± 0.05^{b}
Succinic acid (mg/g)	0.11 ± 0.01	ND	ND	ND	ND

Note: ND indicates that the test result is below the device threshold, i.e. not detected, the same below Different lowercase letters represent significant differences in factors at $p < 0.05$.

3.4. Dynamic Changes in Amino Acids in WHDS during Ripening

Amino acids are the basic units of proteins and the main flavour substances of many foods. There are nine essential amino acids, namely, Lys, Trp, Phe, Met, Thr, Val, Ile, Leu, and Tyr, and vegetables and fruits are the main sources of amino acid intake for the human body [42]. The 17 common amino acids are usually classified as umami amino acids (UAAs), sweet amino acids (SAAs), bitter amino acids (BAAs), and Others. Asp and Glu belong to UAAs; Gly, Trp, Ala, Pro, Ser, Met, and Thr belong to SAAs; Val, Leu, Phe, Lys, Ile, and Arg belong to BAAs; and the remaining Tyr and Cys belong to Others [43]. The composition of flavour-presenting amino acids directly affects the quality and taste of mulberry fruit, so changes in the flavour-presenting amino acid composition were examined during ripening [44]. As shown in Figure 3a, UAAs showed a slow decline from 26% to 23% as WHDS matured. The content of SAAs was not stable throughout the stage, but varied little from stage to stage, with a maximum of 36% at S2 and S4. There was no clear pattern in the variation in BAAs, with the peak of 38% occurring at S5. The contents of the other amino acids did not change throughout the ripening stage and were all 5%. Among the first three types of flavour-presenting amino acids, SAAs and UAAs are the most important components of mulberry flavour, and although the contents of the two flavour-presenting amino acids tended to decrease with the increase in ripening, the content of these two types of amino acids accounted for more than 56% of the total content at all stages and reached the maximum value of 61% in S2. The high proportion of SAAs and UAAs improves the flavour profile of WHDS as well as the nutritional value.

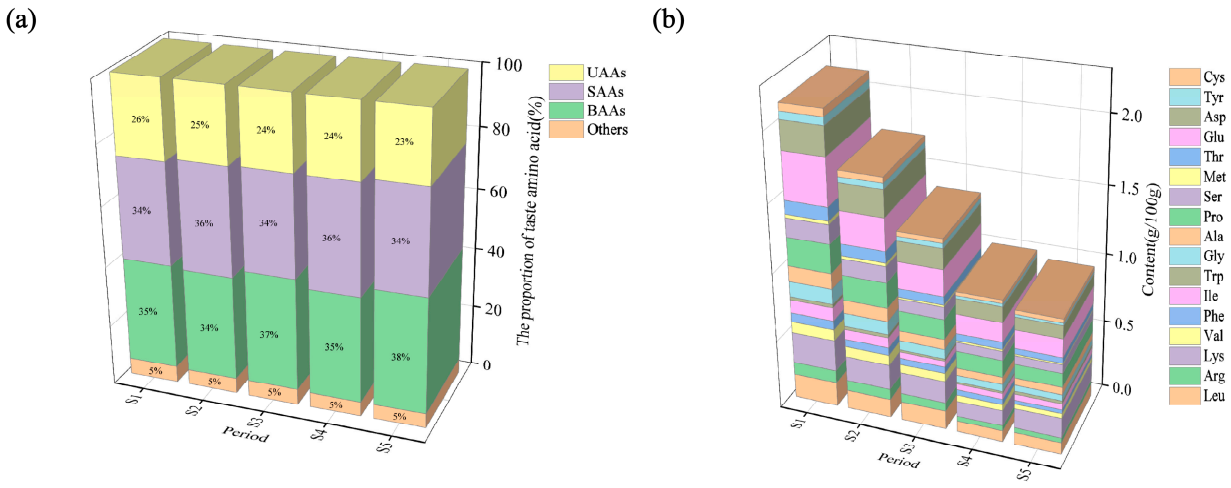


Figure 3. Alterations in the proportion of taste amino acids at different maturity stages of WHDS (**a**) and alterations in the amino acid composition (**b**).

The composition of the three flavour-presenting amino acids is not sufficient to provide a full picture of the quality and taste of WHDS but needs to be evaluated in relation to the content of the individual free amino acids. The type and content of free amino acids in mulberries are affected by various factors, such as the variety, soil, and water [45,46]. As shown in Figure 3b, 17 free amino acids were detected during the maturation of WHDS, and the amino acids with the highest and lowest levels were Glu and Trp at 0.347 ± 0.032 g/100 g and 0.024 ± 0.002 g/100 g, respectively. The total amino acid content ranged from 0.976 ± 0.233 g/100g to 2.142 ± 0.131 g/100g, showing a decreasing trend, and the amino acids with a decrease rate of more than 60% were Tyr, Glu, Gly, and Arg, while the rest of the amino acids showed a decrease rate of less than 60%. Volatile aromatic substances such as alcohols, aldehydes, ketones, and esters during fruit ripening are mainly metabolised by the amino acids Val, Leu, Ile, and Phe [47], which explains the decrease in the total amino acids with ripening.

3.5. Dynamic Changes in Mineral Content in WHDS during Ripening

Mulberries are rich and well balanced in terms of minerals and have good nutritional potential, making them suitable as a food source for mineral supplementation in the daily diet [48]. In the experiment, ICP-MS was used to determine changes in the total contents of four minerals (i.e., Ca, K, Fe, and Se) during the WHDS maturation process, and the results are shown in Figure 4. During the maturation process, Se showed an increasing and then decreasing trend, while the remaining three minerals showed irregular trends. K is an important component of the body's electrolytes, an imbalance of which can cause an abnormal heart rate and, in severe cases, can lead to shock or even death [49]. As shown in Figure 4a, the K in WHDS was highest in S1 at 3019.52 ± 77.99 mg/L and then reached its lowest value in S4 at 2061.73 ± 31.69 mg/L. Ca is an essential mineral for the human body, and, as shown in Figure 4b, the Ca content presented an overall decreasing trend, with 1617.86 ± 24.45 mg/L in S1 and 823.137 ± 9.54 mg/L in S5; therefore, WHDS in S1 may be a good choice for Ca-deficient patients. Fe and Se are trace elements in the body, and deficiencies in these two minerals may lead to the impaired function of bone-forming cells (e.g., osteoblasts and osteoclasts), thus affecting bone density and quality [50]. As shown in Figure 4c,d, the Fe and Se contents were not very high, with Fe concentrations ranging from 10.87 ± 0.45 mg/L to 33.50 ± 0.66 mg/L and Se concentrations ranging from 0.43 ± 0.01 mg/L to 0.34 ± 0.00 mg/L. In terms of the overall content, K was the highest, followed by Ca, Fe, and Se in descending order, and all four minerals decreased to varying degrees from S1 to S5, which is very similar to the results of previous studies on mulberry [14]. It is speculated that the reason for this observation may be that, during the ripening process of mulberries, minerals may be converted into other forms of organic acids and vitamins.

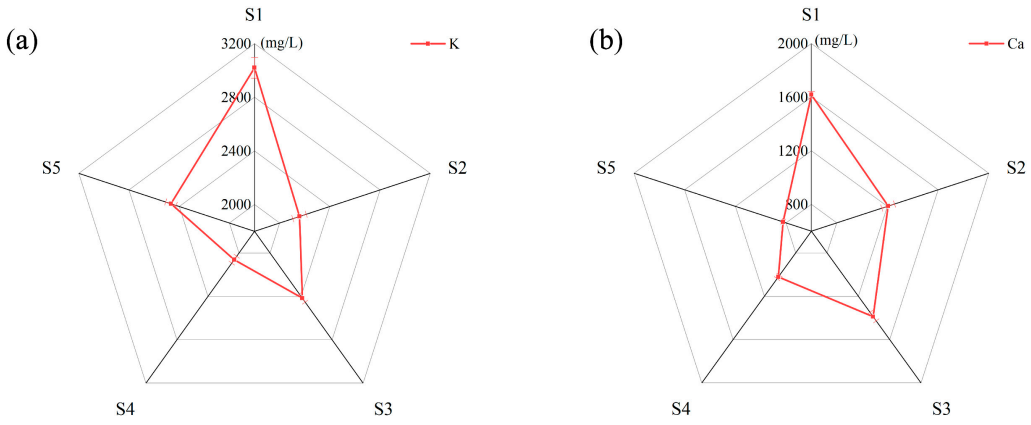


Figure 4. *Cont.*

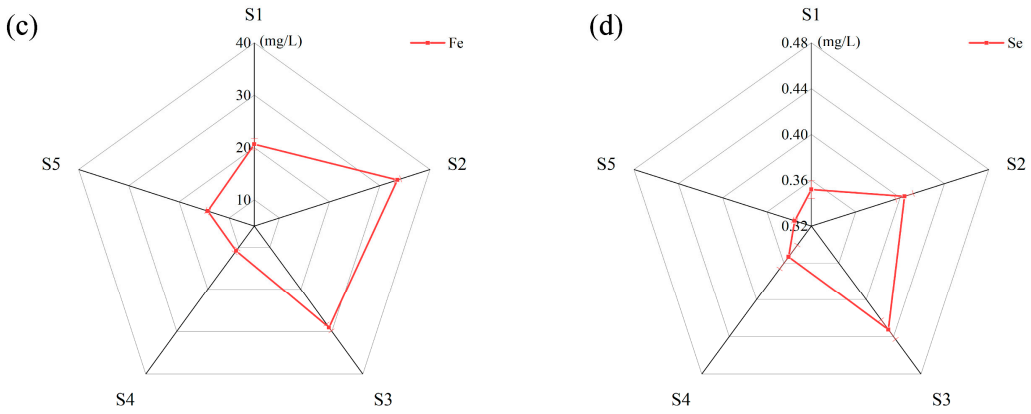


Figure 4. Radar map display of the K (**a**), Ca (**b**), Fe (**c**), and Se (**d**) in WHDS at different maturity stages.

3.6. Dynamic Changes in Volatile Flavour Compounds in WHDS during Ripening

The aroma composition of mulberry is complex and mainly derived from the metabolic decomposition of fatty acids, amino acids, and other precursors, the type and content of which will be affected by the variety, maturity, and growth environment [51]. As can be seen in Table 3, a total of 26 volatile flavour substances were detected during the maturation process of WHDS, including eight esters, seven alcohols, four acids, three aldehydes, two ketones, and one each of phenols and terpenes. The total content of volatile flavour substances increased with the maturation degree and basically reached a stable level at S4, with the total content in the range of 209.09 ± 4.92 mg/L to 1279.09 ± 33.50 mg/L.

Alcohols, at 59–69%, are the main source of WHDS aroma, mainly 2,3-butanediol, 3-Methyl-1-butanol, and 1,2,3-Propanetriol. These higher alcohols not only act as precursors to esters, but also give WHDS a rosy, herbaceous, and oily bark flavour to increase the body [52,53]. The largest variety of esters, most of which are derived from esterification reactions, contribute significantly to flavour formation in WHDS. Ethyl butyrate, ethyl benzoate, and methyl caproate are the more common volatiles of the five stages, which can give WHDS a more pineapple and grassy aroma, and the ethyl caproate and ethyl propionate generated in S4 and S5 can increase its sweetness and fruity taste [54]. Ethyl propionate and ethyl valerate were only detected in the pre-ripening stage. Acids, which are also precursors of esters [55], are the main constituents of the mulberry aroma. The content of acetic and butyric acids increased with maturity, with lactic and acetic acids gradually appearing in the later stages of ripening. Aldehydes and ketones are fewer in variety and lower in content, but they are also an important part of the mulberry aroma. Amino acids are an important source of aldehydes [56], and high concentrations of alcohols also increase aldehydes under aerobic conditions [57]. The detected compounds isovaleraldehyde, furfural, phenylacetaldehyde, and 3-hydroxydibutanone reduce oral and oesophageal irritation [58] and enhance the softness of the WHDS taste. Terpenediene and phenol also optimise the aroma and flavour of WHDS.

In addition, we performed PCA and categorised the flavour substances for the five stages, and the results are shown in Figure 5. As shown in Figure 5a, the total explanation of the two principal components is 88.0%, and, according to the division of RDA1 and RDA2, S1 and S2 are in the third quadrant, S3 is in the second quadrant, S4 is in the fourth quadrant, and S5 is in the first quadrant, with no overlap among any of the stages, which suggests that there is a high degree of variability among the five maturity stages. In terms of the area covered, the S4 stage was the most extensive, indicating the greatest variety of flavour substances at 22, which is in keeping with the findings shown in Figure 5b. Studies have shown that there are significant differences in the flavour substances of WHDS at different ripening stages, and the scientific and rational harvesting of fruits at different stages can ensure the edible quality and nutritional value of WHDS and is conducive to further processing.

Table 3. Dynamic changes in volatile flavour substances in WHDS during ripening.

No.	Compounds	S1	S2	S3	S4	S5
	Alcohols					
1	3-Methyl-1-butanol	15.63 ± 0.37^{e}	55.27 ± 2.00^{d}	72.27 ± 2.14^{c}	164.53 ± 7.03^{b}	176.34 ± 7.89^{a}
2	2-Octanol	32.02 ± 0.84^{d}	32.03 ± 0.43^{d}	91.03 ± 3.00^{b}	61.20 ± 0.80^{c}	114.10 ± 5.90^{a}
3	2,3-Butanediol	40.45 ± 1.60^{e}	117.20 ± 3.61^{d}	149.98 ± 3.89^{c}	343.12 ± 8.89^{b}	371.44 ± 13.43^{a}
4	Terpineol	ND	ND	ND	12.08 ± 0.20	ND
5	Propanediol	ND	ND	ND	ND	9.21 ± 0.18
6	1,2,3-Propanetriol	40.16 ± 0.68^{e}	95.96 ± 2.24^{d}	119.05 ± 2.81^{c}	156.10 ± 7.18^{b}	144.73 ± 1.94^{a}
7	Phenethyl alcohol	2.76 ± 0.07^{e}	13.20 ± 0.32^{d}	15.39 ± 0.36^{c}	33.37 ± 0.77^{a}	16.92 ± 0.67^{b}
	Acids					
8	Acetic acid	33.65 ± 0.54^{d}	68.79 ± 2.07^{c}	98.03 ± 2.58^{b}	124.53 ± 0.42^{a}	124.56 ± 1.25^{a}
9	Butyric acid	5.93 ± 0.10^{d}	ND	8.58 ± 0.14^{c}	32.36 ± 0.79^{a}	10.98 ± 0.18^{b}
10	Lactic acid	ND	ND	ND	65.79 ± 1.48^{a}	8.06 ± 0.14^{b}
11	Caproic acid	ND	ND	11.76 ± 0.20^{c}	24.26 ± 0.58^{a}	17.88 ± 0.53^{b}
	Aldehydes					
12	Isovaleric aldehyde	3.74 ± 0.09^{e}	11.97 ± 0.24^{d}	19.77 ± 0.27^{c}	36.02 ± 0.85^{b}	37.15 ± 0.63^{a}
13	Furfural	1.88 ± 0.03^{d}	2.27 ± 0.07^{c}	2.55 ± 0.02^{c}	7.81 ± 0.38^{a}	3.63 ± 0.08^{b}
14	Phenylacetaldehyde	1.72 ± 0.02^{d}	1.99 ± 0.10^{d}	5.10 ± 0.11^{c}	8.29 ± 0.11^{b}	9.14 ± 0.39^{a}
	Ketones					
15	3-Hydroxydibutanone	4.06 ± 0.04^{e}	11.73 ± 0.39^{d}	17.26 ± 0.06^{c}	37.51 ± 0.79^{a}	32.71 ± 1.12^{b}
16	Hydroxyacetone	ND	ND	ND	15.40 ± 0.41	ND
	Esters					
17	Ethyl formate	ND	3.37 ± 0.06	ND	ND	ND
18	Ethyl butyrate	1.56 ± 0.03^{e}	4.83 ± 0.09^{c}	4.06 ± 0.14^{d}	8.13 ± 0.19^{b}	11.97 ± 0.16^{a}
19	Ethyl acetate	ND	19.03 ± 0.44^{c}	26.91 ± 0.79^{b}	53.23 ± 0.92^{a}	53.61 ± 0.71^{a}
20	Ethyl benzoate	1.40 ± 0.04^{e}	3.00 ± 0.02^{d}	6.26 ± 0.13^{c}	8.89 ± 0.09^{a}	7.80 ± 0.15^{b}
21	Methyl hexanoate	3.00 ± 0.06^{e}	10.89 ± 0.49^{d}	21.82 ± 0.64^{c}	27.68 ± 0.58^{a}	23.66 ± 0.66^{b}
22	Ethyl caproate	2.51 ± 0.04^{b}	ND	ND	13.71 ± 0.42^{a}	ND
23	Ethyl propionate	6.55 ± 0.11^{b}	ND	ND	ND	41.90 ± 0.96^{a}
24	Ethyl valerate	1.80 ± 0.03^{a}	3.66 ± 0.06^{b}	ND	ND	ND
	Others					
25	Phenol	1.21 ± 0.02^{b}	ND	6.02 ± 0.22^{a}	ND	ND
26	Terpenediene	9.06 ± 0.21^{b}	ND	44.34 ± 0.75^{a}	45.08 ± 0.62^{a}	44.24 ± 1.35^{a}

Note: Different lowercase letters represent significant differences in factors at $p < 0.05$.

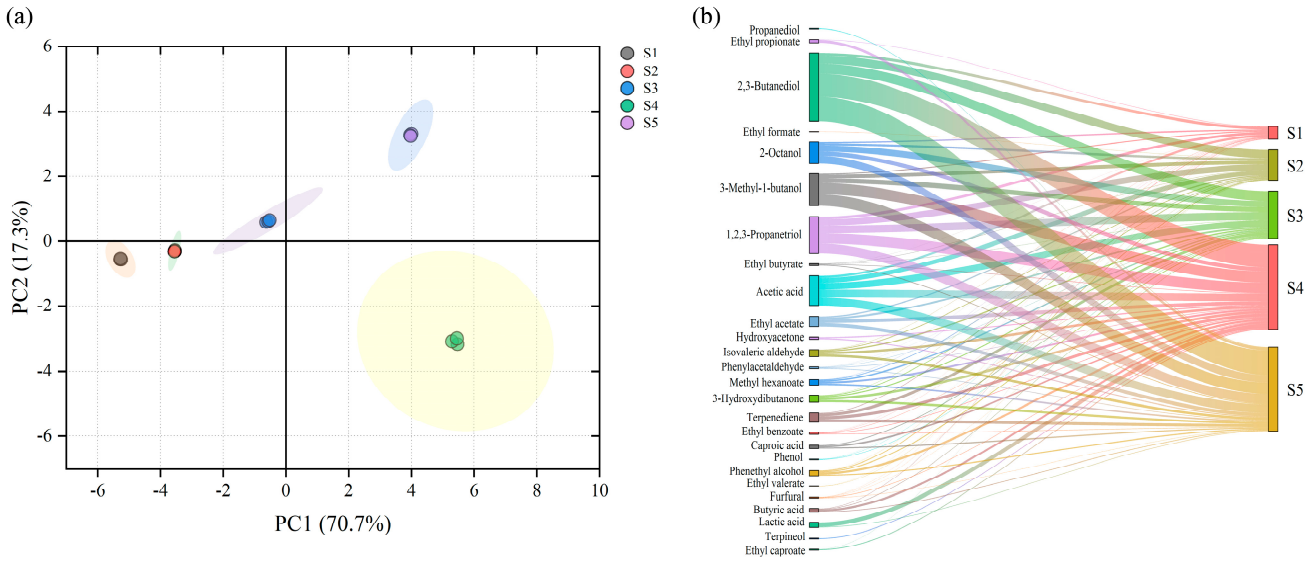


Figure 5. Principal component analysis (PCA) (**a**) and Sankey diagram (**b**) of volatile components at different maturity stages of WHDS.

3.7. Dynamic Changes in Community Structures in WHDS during Ripening

There is a close correlation between microbial community structure and plant growth. The high-throughput sequencing of micro-organisms at different maturation stages of WHDS was performed using the Illumina MiSeq PE300 microbial detection platform to determine the succession of micro-organisms on its surface. The test results yielded a total of 521,485 valid sequences, with an average of 104,297 sequences per sample and a total of 1647 OTUs divided by 97% similarity, which were mainly concentrated in the interval length of 361–380 bp. The statistics of the number of taxonomic units after OTU clustering were 1 domain, 1 kingdom, 12 phyla, 19 orders, 56 orders, 101 families, 190 genera, and 242 species. As shown in Figure 6a, the bacterial communities in the different maturation stages of WHDS consisted of *Proteobacteria*, *Actinobacteriota*, *Firmicutes*, *unclassified norank Bacteria*, *Bacteroidota*, *Myxococcota*, *Deinococcota*, *Chloroflexi*, *Verrucomicrobiota*, *Abditibacteriota*, and Others. Among them, *Proteobacteria*, *Actinobacteriota*, *Firmicutes*, and *unclassified norank bacteria* were the dominant genera and equally present in other fruits [59,60], while the relative abundance of the other 12 phyla was below 1%. It can also be seen in Figure 6a that the relative abundance of *Proteobacteria* showed a significant increasing trend with increasing maturity, from 10.82% to 65.89% and, finally, 75.51%. The relative abundance of *Actinobacteriota* decreased from 52.14% to 11.78% and that of *Firmicutes* from 35.68% to 11.30%, with both abundances decreasing significantly. *Unclassified norank bacteria* varied less throughout the stage, at around 1%. It is worth noting that *unclassified norank bacteria* have been less studied in previous articles, and their specific functional properties and metabolic mechanisms need to be further examined.

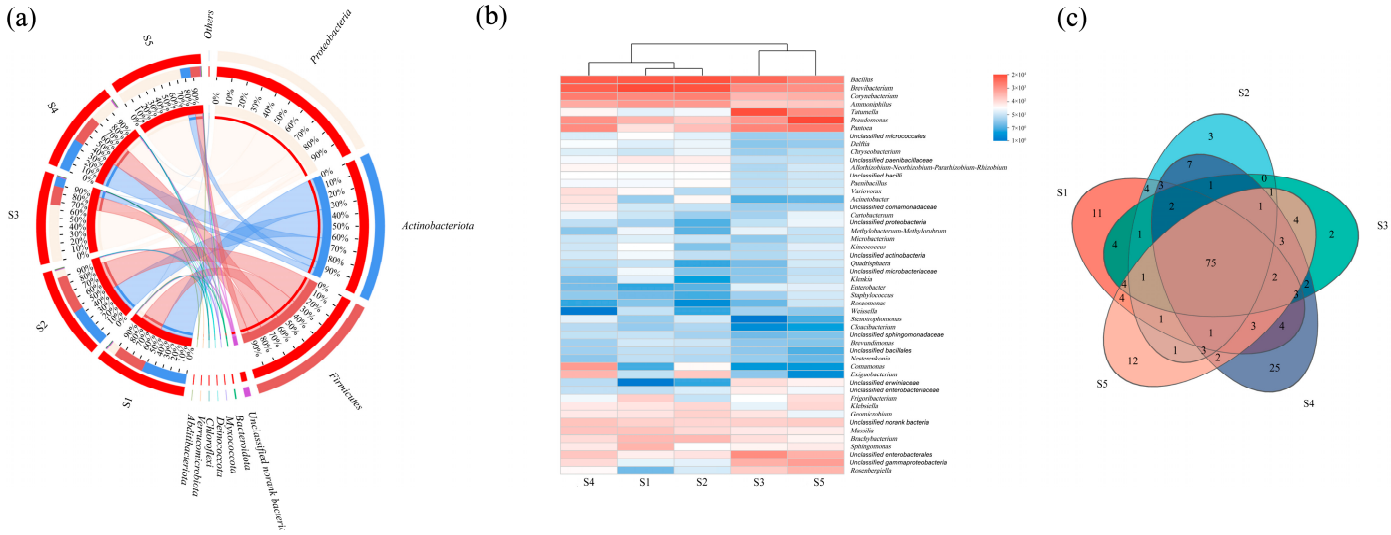


Figure 6. Microbial community (**a**), heat map (**b**), and Venn diagram (**c**) at different maturity stages of WHDS. Note: the numbers in (**c**) indicate the species of strains common to certain stages.

In addition, as can be seen in Figures 6b,c, S3 and S5 clustered into one group, and the remaining three stages clustered into one group. A total of 123 bacterial genera were present in S1, 105 bacterial genera were present in S2, 104 bacterial genera were present in S3, 112 bacterial genera were present in S4, and 118 bacterial genera were present in S5, with no regular trend in the number of genera. The common dominant bacterial genera were *Bacillus* (9.1%–34.95%), *Brevibacterium* (6.46%–38.94%), *Pseudomonas* (1.25%–42.16%), *Tatumella* (0.18%–37.15%), *Corynebacterium* (2.21%–11.19%), *Pantoea* (0.69%–12.12%), *Ammoniphilus* (1.22%–5.29%), *Unclassified enterobacterales* (0.66%–7.07%), *Unclassified gammaproteobacteria* (0.49%–4.44%), and *Brachybacterium* (1.07%–2.13%). *Bacillus* changes in relative abundance as it increases in maturity, first increasing and then decreasing. Some species of *Bacillus*, like *Bacillus cereus NRKT*, are important biological control bacteria to reduce the fruit ripe rot disease caused by *Colletotrichum gloeosporioides* [61], and these genera have been

detected in soil where fruits are grown [62]. The trend of *Bacillus subtilis* was similar to that of *Bacillus*. *Bacillus subtilis* is an effective genus of biocontrol organisms [63], and spraying it as a solution on fruit vines was effective in increasing the alcohol and ester content of the corresponding fruit wines [64]. The abundance of *Pseudomonas* showed an increasing trend, reaching a maximum at S5. *Pseudomonas* can have beneficial effects on plants, such as nitrogen fixation and phosphorus solubilisation, as well as in other diseases, such as spotting [65,66]. *Corynebacterium* uses glucose to produce methyl anthranilate, which significantly enhances the flavour of fruits [67]. *Tatumella* and *Pantoea* are important components of the WHDS microbial community and enhance total biogenic amines when they act as dominant genera [58]. The remaining four dominant genera have been studied relatively little, and the mechanisms of their effects on WHDS need to be explored in further designed experiments.

In summary, the microbial community structure in WHDS at different maturity levels varied considerably, and the microbial community structure was closely related to fruit flavour. The community structure at each stage was analysed with the aim of obtaining key genera that can regulate fruit flavour, which is important for improving the quality of mulberries at different maturity levels.

3.8. Correlation Analysis

In order to further clarify the relationship between microbial communities and physicochemical properties and flavour substance species during mulberry ripening, a Spearman ($|\rho| > 0.5$ and $p < 0.05$)-based co-occurrence network analysis of micro-organisms at the level of WHDS genera was carried out, and the results are shown in Figure 7.

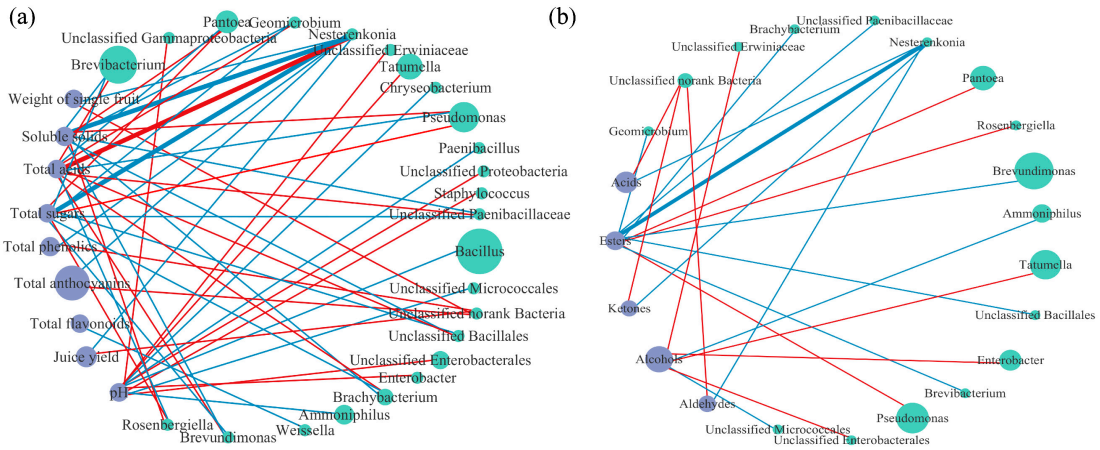


Figure 7. Correlation network analysis of differential micro-organisms and physiological indicators (**a**) and flavour substance type (**b**).

As can be seen in Figure 7a, 24 micro-organisms and 9 physicochemical properties were significantly correlated. *Nesterenkonia*, a bacterium that has been detected on the leaves of non-organic grapes [68], was the most highly associated micro-organism, with highly significant positive correlations with total acid ($p < 0.01$), significant negative correlations with the weight of single fruit, juice yield, total phenolics, and total flavonoids, and highly significant negative correlations with soluble solids and total sugar ($p < 0.01$). pH was the most highly correlated physicochemical property, with significant negative correlations with *Ammoniphilus*, *Bacillus*, *Paenibacillus*, *Chryseobacterium*, and *Unclassified Micrococcales*, and significant positive correlations with *Unclassified Proteobacteria*, *Unclassified Erwiniaceae*, *Unclassified Gammaproteobacteria*, *Unclassified Enterobacterales*, *Tatumella*, *Enterobacter*, and *Staphylococcus*. Apart from this, total flavonoid content was significantly negatively correlated with *Weissella*. The juice yield, weight of single fruit, total phenolics, and total anthocyanins were significantly and positively correlated with *Unclassified norank*

Bacteria. Soluble solids and total sugars were significantly negatively correlated with most micro-organisms.

As can be seen in Figure 7b, 17 micro-organisms and 5 flavour substance species were significantly correlated. As in Figure 7a, *Nesterenkonia* was, again, the most highly associated micro-organism, with significant negative correlations with the four flavour substance species and, in particular, a highly significant negative correlation ($p < 0.01$) with esters. The esters category was the most highly correlated flavour substance type, with significant negative correlations with *Brevibacterium*, *Brachybacterium*, *Geomicrobium*, *Unclassified Paenibacillaceae*, *Brevundimonas*, and *Unclassified Bacillales*, and significant positive correlations with *Pseudomonas*, *Pantoea*, and *Rosenbergiella* [69]. In addition to this, acids, ketones, and aldehydes were significantly positively correlated with *Unclassified norank Bacteria*, while the alcohols category was significantly negatively correlated with *Ammoniphilus* and *Unclassified Micrococcales* and significantly positively correlated with *Tatumella*, *Unclassified Enterobacterales*, *Unclassified Erwiniaceae*, and *Enterobacter.*

4. Conclusions

Due to the open growth environment and dynamic growth process, the physicochemical properties, antioxidant capacity, minerals, organic acids, amino acids, volatile flavour substances, and microbial communities during mulberry ripening showed significant diversity and dynamics. In this study, we found that under-ripe WHDS contained more amino acids and organic acids, whereas ripe mulberries were enriched with more phenolic compounds and were therefore more suitable for consumption. At the same time, we pinpointed the bacterial community structure during the WHDS maturation process, comprehensively analysed the correlations between the dominant bacterial community and the physicochemical properties and flavour substance species, and revealed the succession pattern of the bacterial community structure and its correlation with the physicochemical properties and flavour substance species. The reported findings provide a theoretical reference for further exploring the potential nutritional value of mulberry and optimising its quality and taste. However, this study only focused on the dominant genera during the WHDS ripening process and did not investigate the low-abundance genera in detail, but they may have a positive impact on aspects such as physicochemical properties and flavour substances as the ripening process progresses. In the future, combining next-generation sequencing technology and more comprehensive theoretical knowledge, the growing environment of mulberry and the biological characteristics of different micro-organisms should be used as a starting point to further isolate and functionally validate different mulberry varieties and micro-organisms of medium and low abundance.

Supplementary Materials: The following supporting information can be downloaded at: https://www.mdpi.com/article/10.3390/agriculture14071129/s1, Table S1. Quantitative parameters of organic acid standards. Table S2. Quantitative parameters of amino acid standards. Figure S1. The internal standard of flavour substances investigated in this work.

Author Contributions: Conceptualisation, experiment, software, writing—original draft, writing—review and editing, Y.F. (Yuli Fang); writing—original draft, methodology, data curation, writing—review and editing, validation, M.B.; supervision, project administration, writing—review and editing, validation, T.Y.; supervision, writing—review and editing, validation, Q.X.; writing—review and editing, data interpretation, Y.X.; data curation, software, data collection, H.T. (Hongyi Tang); literature search, validation, data interpretation, Y.F. (Yiling Feng); funding acquisition, writing—review and editing, supervision, project administration, B.H. All authors have read and agreed to the published version of the manuscript.

Funding: This work was supported by the 2023 Luzhou Laojiao Graduate Student Innovation Fund (LJCX2023-6) and the Nanchong Science and Technology Plan Project (21CGZH0013).

Data Availability Statement: The original contributions presented in the study are included in the article/supplementary material. Further inquiries can be directed to the corresponding author.

Conflicts of Interest: The authors declare that the submitted work was carried out in the absence of any personal, professional, or financial relationships that could potentially be construed as conflicts of interest.

References

1. Ma, D.; Lin, T.; Zhao, H.; Li, Y.; Wang, X.; Di, S.; Liu, Z.; Liu, M.; Qi, P.; Zhang, S.; et al. Development and comprehensive SBSE-GC/Q-TOF-MS analysis optimization, comparison, and evaluation of different mulberry varieties volatile flavor. *Food Chem.* **2024**, *443*, 138578. [CrossRef]
2. Li, R.; Wang, J.; Liu, J.; Li, M.; Lu, J.; Zhou, J.; Zhang, M.; Ferri, N.; Chen, H. Mulberry leaf and its effects against obesity: A systematic review of phytochemistry, molecular mechanisms and applications. *Phytomedicine* **2024**, *128*, 155528. [CrossRef]
3. Ali Redha, A.; Freije, A.; Kodikara, C.; Rondanelli, M.; Aqeel, E.; Zafar, W.; Albunni, H.; Merza, H.; Khonji, A.; Aljar, M.; et al. Comparison of fatty acid profile and mineral content of black mulberry (*Morus nigra*), white mulberry (*Morus alba*) and red mulberry (Morus rubra) grown in Bahrain. *Appl. Food Res.* **2023**, *3*, 100358. [CrossRef]
4. Kattil, A.; Hamid; Dash, K.K.; Shams, R.; Sharma, S. Nutritional composition, phytochemical extraction, and pharmacological potential of mulberry: A comprehensive review. *Future Foods* **2024**, *9*, 100295. [CrossRef]
5. Wang, P.-Y.; Shuang, F.-F.; Yang, J.-X.; Jv, Y.-X.; Hu, R.-Z.; Chen, T.; Yao, X.-H.; Zhao, W.-G.; Liu, L.; Zhang, D.-Y. A rapid and efficient method of microwave-assisted extraction and hydrolysis and automatic amino acid analyzer determination of 17 amino acids from mulberry leaves. *Ind. Crops Prod.* **2022**, *186*, 115271. [CrossRef]
6. Venkatesh Kumar, R.; Vyry, W.N.A.; Chauhan, S.; Singh, V.; Srivastava, D.; Kumar, U.; Raj, R.; Verma, A. Mulberry: From nutraceuticals to bioactive phytochemicals. *Food Humanit.* **2024**, *2*, 100272. [CrossRef]
7. Zhong, S.; Yang, Y.; Huo, J.; Sun, Y.; Ren, N.; Lu, Q.; Li, D.; Zhan, P.; Wu, W.; Chen, H.; et al. Dissection of gut microbiota and metabolites reveals the hypolipidemic effect of green mulberry leaf tea / black mulberry leaf tea in mice. *J. Funct. Foods* **2023**, *111*, 105906. [CrossRef]
8. Choosung, P.; Utto, W.; Boonyaritthongchai, P.; Wasusri, T.; Wongs-Aree, C. Ethanol vapor releasing sachet reduces decay and improves aroma attributes in mulberry fruit. *Food Packag. Shelf Life* **2019**, *22*, 100398. [CrossRef]
9. Wang, K.; Qi, J.; Jin, Y.; Li, F.; Wang, J.; Xu, H. Influence of fruit maturity and lactic fermentation on physicochemical properties, phenolics, volatiles, and sensory of mulberry juice. *Food Biosci.* **2022**, *48*, 101782. [CrossRef]
10. de Sousa Fontes, V.M.; Colombo Pimentel, T.; Martins da Silva, A.B.; Suely Madruga, M.; Magnani, M.; dos Santos Lima, M. An improved method for determining free amino acids by RP-HPLC/DAD with o-phthalaldehyde derivatization: Method evaluation in beers and wines. *Food Chem.* **2024**, *435*, 137591. [CrossRef]
11. Lan, L.; Wang, J.; Wang, S.; He, Q.; Wei, R.; Sun, Z.; Duan, S.; Li, Y. Correlation between microbial community succession and flavor substances during fermentation of Yongchuan Douchi. *Food Biosci.* **2023**, *56*, 103192. [CrossRef]
12. Zhu, J.; Wang, L.; Xiao, Z.; Niu, Y. Characterization of the key aroma compounds in mulberry fruits by application of gas chromatography–olfactometry (GC-O), odor activity value (OAV), gas chromatography-mass spectrometry (GC–MS) and flame photometric detection (FPD). *Food Chem.* **2018**, *245*, 775–785. [CrossRef] [PubMed]
13. Ma, D.; Zhao, H.; Liu, Z.; Liu, M.; Qi, P.; Di, S.; Zhang, S.; Wang, X. Recent advances on mulberry volatile flavor: A review. *J. Food Compos. Anal.* **2023**, *124*, 105665. [CrossRef]
14. Lin, M.; Li, Y.; Gao, Q.; Shi, L.; He, W.; Li, W.; Liang, Y.; Zhang, Z. Dynamic changes in physicochemical and transcriptional expression profiles of mulberry (*Morus alba* L.) fruit during ripening. *Food Biosci.* **2024**, *57*, 103606. [CrossRef]
15. Hu, L.; Wang, C.; Guo, X.; Chen, D.; Zhou, W.; Chen, X.; Zhang, Q. Flavonoid Levels and Antioxidant Capacity of Mulberry Leaves: Effects of Growth Period and Drying Methods. *Front. Plant Sci.* **2021**, *12*, 684974. [CrossRef] [PubMed]
16. *GB/T 15038-2006*; State Administration for Market Supervision and Administration China National Standardization Administration, General Methods of Analysis for Wines and Fruit Wines. China Standard Press: Beijing, China, 2006.
17. Liu, J.; Wan, Y.; Chen, Y.; Li, M.; Liu, N.; Luo, H.; Huang, D.; Peng, H.; Fu, G. Effects of Torulaspora delbrueckii on physicochemical properties and volatile flavor compounds of navel orange wine. *J. Food Compos. Anal.* **2023**, *121*, 105328. [CrossRef]
18. Xia, H.; Zhang, X.; Shen, Y.; Guo, Y.; Wang, T.; Wang, J.; Lin, L.; Deng, H.; Deng, Q.; Xu, K.; et al. Comparative analysis of flavonoids in white and red table grape cultivars during ripening by widely targeted metabolome and transcript levels. *J. Food Sci.* **2022**, *87*, 1650–1661. [CrossRef] [PubMed]
19. Wang, C.; Lu, Y.; Li, Z.; An, X.; Gao, Z.; Tian, S. Preparation and Performance Characterization of a Composite Film Based on Corn Starch, κ-Carrageenan, and Ethanol Extract of Onion Skin. *Polymers* **2022**, *14*, 2986. [CrossRef] [PubMed]
20. Zhou, H.; Wang, S.; Liu, W.; Chang, L.; Zhu, X.; Mu, G.; Qian, F. Probiotic properties of Lactobacillus paraplantarum LS-5 and its effect on antioxidant activity of fermented sauerkraut. *Food Biosci.* **2023**, *52*, 102489. [CrossRef]
21. Scutarașu, E.C.; Teliban, I.V.; Zamfir, C.I.; Luchian, C.E.; Colibaba, L.C.; Niculaua, M.; Cotea, V.V. Effect of Different Winemaking Conditions on Organic Acids Compounds of White Wines. *Foods* **2021**, *10*, 2569. [CrossRef]
22. Xu, W.; Zhong, C.; Zou, C.; Wang, B.; Zhang, N. Analytical methods for amino acid determination in organisms. *Amino Acids* **2020**, *52*, 1071–1088. [CrossRef]
23. Shimizu, H.; Akamatsu, F.; Kamada, A.; Koyama, K.; Iwashita, K.; Goto-Yamamoto, N. Effects of variety and vintage on the minerals of grape juice from a single vineyard. *J. Food Compos. Anal.* **2022**, *107*, 104377. [CrossRef]

24. Ji, X. Comparative investigation of volatile components and bioactive compounds in beers by multivariate analysis. *Flavour Fragr. J.* **2021**, *36*, 374–383. [CrossRef]
25. Yilmaz, T.; Ates, F.; Turan, M.; Hatterman-Valenti, H.; Kaya, O. Dynamics of Sugars, Organic Acids, Hormones, and Antioxidants in Grape Varieties 'Italia' and 'Bronx Seedless' during Berry Development and Ripening. *Horticulturae* **2024**, *10*, 229. [CrossRef]
26. Xu, K.; Fan, G.; Wu, C.; Suo, A.; Wu, Z. Preparation of anthocyanin-rich mulberry juice by microwave-ultrasonic combined pretreatment. *Food Sci. Biotechnol.* **2022**, *31*, 1571–1581. [CrossRef]
27. Šarac, D.P.; Tremmel, M.; Vujetić, J.; Torović, L.; Orčić, D.; Popović, L.; Mimica-Dukić, N. Lesjak How do in vitro digestion and cell metabolism affect the biological activity and phenolic profile of grape juice and wine. *Food Chem.* **2024**, *449*, 139228. [CrossRef]
28. Ahmed, M.; Bose, I.; Goksen, G.; Roy, S. Himalayan Sources of Anthocyanins and Its Multifunctional Applications: A Review. *Foods* **2023**, *12*, 2203. [CrossRef]
29. Shipp, J.; Abdel-Aal, E.S.M. Food Applications andPhysiological Effects of Anthocyanins as Functional Food Ingredients. *Open Food Sci. J.* **2010**, *4*, 7–22. [CrossRef]
30. Tang, R.; He, Y.; Fan, K. Recent advances in stability improvement of anthocyanins by efficient methods and its application in food intelligent packaging: A review. *Food Biosci.* **2023**, *56*, 103164. [CrossRef]
31. Wu, L.; Wang, F.; Sha, R.; Li, X.; Yu, K.; Feng, J. The Effect of N and KH2PO4 on Skin Color, Sugars, and Organic Acids of "Flame Seedless" Grape. *Agronomy* **2023**, *13*, 902. [CrossRef]
32. Chaudhary, N.; Roy, Z.; Bansal, R.; Siddiqui, L. Understanding the Role of Free Radicals and Antioxidant Enzymes in Human Diseases. *Curr. Pharm. Biotechnol.* **2023**, *24*, 1265–1276. [CrossRef]
33. Becker, M.; Nunes, G.; Ribeiro, D.; Silva, F.; Catanante, G.; Marty, J.L. Determination of the Antioxidant Capacity of Red Fruits by Miniaturized Spectrophotometry Assays. *J. Braz. Chem. Soc.* **2019**, *30*, 1108–1114. [CrossRef]
34. Hosen, M.Z.; Biswas, A.; Islam, M.R.; Bhuiyan, M.N.I.; Hossain, S.J. Comparison of physicochemical and antioxidant properties of edible fruits in the Sundarbans' mangrove forest, Bangladesh. *Bangladesh J. Bot.* **2020**, *49*, 671–678. [CrossRef]
35. Prakash, O.; Supriya, A.; Kudachikar, V.B. Physicochemical Changes, Phenolic Profile and Antioxidant Capacities of Colored and White Grape (*Vitis vinifera* L.) Varieties during Berry Development and Maturity. *Int. J. Fruit Sci.* **2020**, *20*, S1773–S1783. [CrossRef]
36. Cetin, B.E.; Saraçoğlu, O. Effects of Different Maturity Stages and Fruit Parts on Quality Traits of Plum (Prunus domestica) Fruits. *Erwerbs-Obstbau* **2022**, *65*, 1069–1077. [CrossRef]
37. Li, M.; Su, J.; Yang, H.; Feng, L.; Wang, M.; Xu, G.; Shao, J.; Ma, C. Grape Tartaric Acid: Chemistry, Function, Metabolism, and Regulation. *Horticulturae* **2023**, *9*, 1173. [CrossRef]
38. Amiri, S.; Nicknam, Z.; Radi, M.; Sayadi, M.; Bagheri, F.; Karimi Khorrami, N.; Abedi, E. Postharvest quality of orange fruit as influenced by salicylic acid, acetic acid, and carboxymethyl cellulose coating. *J. Food Meas. Charact.* **2021**, *15*, 3912–3930. [CrossRef]
39. Güler, E. Polyphenols, organic acids, and their relationships in red grapes of Vitis vinifera and Isabella (Vitis labrusca) under arid conditions. *Eur. Food Res. Technol.* **2022**, *249*, 913–921. [CrossRef]
40. Yu, Y.; Yang, G.; Sun, L.; Song, X.; Bao, Y.; Luo, T.; Wang, J. Comprehensive Evaluation of 24 Red Raspberry Varieties in Northeast China Based on Nutrition and Taste. *Foods* **2022**, *11*, 3232. [CrossRef]
41. Jiang, C.C.; Fang, Z.Z.; Zhou, D.R.; Pan, S.L.; Ye, X.F. Changes in secondary metabolites, organic acids and soluble sugars during the development of plum fruit cv. 'Furongli' (*Prunus salicina* Lindl). *J. Sci. Food Agric.* **2018**, *99*, 1010–1019. [CrossRef]
42. Kudełka, W.; Kowalska, M.; Popis, M. Quality of Soybean Products in Terms of Essential Amino Acids Composition. *Molecules* **2021**, *26*, 5071. [CrossRef]
43. Qian, M.; Ruan, F.; Zhao, W.; Dong, H.; Bai, W.; Li, X.; Liu, X.; Li, Y. Comparison Study of the Physicochemical Properties, Amino Acids, and Volatile Metabolites of Guangdong Hakka Huangjiu. *Foods* **2023**, *12*, 2915. [CrossRef]
44. Xu, L.; Zang, E.; Sun, S.; Li, M. Main flavor compounds and molecular regulation mechanisms in fruits and vegetables. *Crit. Rev. Food Sci. Nutr.* **2022**, *63*, 11859–11879. [CrossRef]
45. Palčić, I.; Korenika, A.M.J.; Jakobović, S.; Pasković, I.; Major, N.; Ban, D.; Ban, S.G.; Karoglan, M.; Petek, M.; Herak Ćustić, M.; et al. Soil type affects grape juice free amino acids profile during ripening of cv. Malvasia Istriana (*Vitis vinifera* L.). *N. Z. J. Crop Hortic. Sci.* **2020**, *48*, 22–33. [CrossRef]
46. Arias-Pérez, I.; Ontañón, I.; Ferreira, V.; Escudero, A. Maturation of Moristel in Different Vineyards: Amino Acid and Aroma Composition of Mistelles and Wines with Particular Emphasis in Strecker Aldehydes. *Foods* **2022**, *11*, 958. [CrossRef]
47. Maoz, I.; Lewinsohn, E.; Gonda, I. Amino acids metabolism as a source for aroma volatiles biosynthesis. *Curr. Opin. Plant Biol.* **2022**, *67*, 102221. [CrossRef]
48. Sun, Z.; Zhou, Y.; Zhu, W.; Yin, Y. Assessment of the Fruit Chemical Characteristics and Antioxidant Activity of Different Mulberry Cultivars (*Morus* spp.) in Semi-Arid, Sandy Regions of China. *Foods* **2023**, *12*, 3495. [CrossRef]
49. McCormick, J.A.; Topf, J.; Tomacruz, I.D.; Grimm, P.R. A New Understanding of Potassium's Influence Upon Human Health and Renal Physiology. *Adv. Kidney Dis. Health* **2023**, *30*, 137–147. [CrossRef]
50. Gaffney-Stomberg, E. The Impact of Trace Minerals on Bone Metabolism. *Biol. Trace Elem. Res.* **2018**, *188*, 26–34. [CrossRef]
51. Mostafa, S.; Wang, Y.; Zeng, W.; Jin, B. Floral Scents and Fruit Aromas: Functions, Compositions, Biosynthesis, and Regulation. *Front. Plant Sci.* **2022**, *13*, 860157. [CrossRef]
52. Chen, L.; Peng, Q.; Liu, B.; Zhang, Y.; Feng, S. Study on the dynamic changes of nutrient components and flavor compounds during the fermentation process of high-quality highland barley wine. *Int. J. Gastron. Food Sci.* **2024**, *35*, 100860. [CrossRef]

53. Qian, Y.L.; An, Y.; Chen, S.; Qian, M.C. Characterization of Qingke liquor aroma from Tibet. *J. Agric. Food Chem.* **2019**, *67*, 13870–13881. [CrossRef]
54. Zhao, Y.; Zhan, P.; Tian, H.-L.; Wang, P.; Lu, C.; Tian, P.; Zhang, Y.-Y. Insights into the Aroma Profile in Three Kiwifruit Varieties by HS-SPME-GC-MS and GC-IMS Coupled with DSA. *Food Anal. Methods* **2021**, *14*, 1033–1042. [CrossRef]
55. Ma, Y.; Li, M.; Zhang, S. Simultaneous Determination of Organic Acids in Chinese Liquor by GC-MS Method. *Asian J. Chem.* **2014**, *26*, 4707–4710. [CrossRef]
56. Chen, L.; Liu, B.; Feng, S.; Ma, X.; Wang, S.; Zhang, Y. Correlation between microbe, physicochemical properties of Jiuqu in different plateau areas and volatile flavor compounds of highland barley alcoholic drink. *Food Biosci.* **2023**, *51*, 102276. [CrossRef]
57. Filipowska, W.; Jaskula-Goiris, B.; Ditrych, M.; Bustillo Trueba, P.; De Rouck, G.; Aerts, G.; Powell, C.; Cook, D.; De Cooman, L. On the contribution of malt quality and the malting process to the formation of beer staling aldehydes: A review. *J. Inst. Brew.* **2021**, *127*, 107–126. [CrossRef]
58. Li, H.; Jiang, D.; Dai, Z.; Zhang, Y.; Zhao, Y. Aromatic property of cherry wine produced by malolactic fermentation of controlled and spontaneous on the bacterial evolution. *Int. J. Food Prop.* **2019**, *22*, 1270–1282. [CrossRef]
59. Zhang, S.; Chen, X.; Zhong, Q.; Zhuang, X.; Bai, Z. Microbial Community Analyses Associated with Nine Varieties of Wine Grape Carposphere Based on High-Throughput Sequencing. *Microorganisms* **2019**, *7*, 668. [CrossRef]
60. Wassermann, B.; Müller, H.; Berg, G. An Apple a Day: Which Bacteria Do We Eat With Organic and Conventional Apples? *Front. Microbiol.* **2019**, *10*, 1629. [CrossRef]
61. Zhang, J.; Wang, E.T.; Singh, R.P.; Guo, C.; Shang, Y.; Chen, J.; Liu, C. Grape berry surface bacterial microbiome: Impact from the varieties and clones in the same vineyard from central China. *J. Appl. Microbiol.* **2019**, *126*, 204–214. [CrossRef]
62. Xu, X.; Miao, Y.; Wang, H.; Du, J.; Wang, C.; Shi, X.; Wang, B. Analysis of Microbial Community Diversity on the Epidermis of Wine Grapes in Manasi's Vineyard, Xinjiang. *Foods* **2022**, *11*, 3174. [CrossRef] [PubMed]
63. Li, Y.; Héloir, M.C.; Zhang, X.; Geissler, M.; Trouvelot, S.; Jacquens, L.; Henkel, M.; Su, X.; Fang, X.; Wang, Q.; et al. Surfactin and fengycin contribute to the protection of a Bacillus subtilis strain against grape downy mildew by both direct effect and defence stimulation. *Mol. Plant Pathol.* **2019**, *20*, 1037–1050. [CrossRef]
64. Malićanin, M.; Danilović, B.; Cvetković, D.; Stamenković-Stojanović, S.; Nikolić, N.; Lazić, M.; Karabegović, I. Modulation of Aroma and Sensory Properties of Prokupac Wines by a Bacillus-based Preparation Applied to Grapes Prior to Harvest. *South Afr. J. Enol. Vitic.* **2020**, *41*, 158–167. [CrossRef]
65. Blumer, C.; Heeb, S.; Pessi, G.; Haas, D. Global GacA-steered control of cyanide and exoprotease production in *Pseudomonas fluorescens* involves specific ribosome binding sites. *Proc. Natl. Acad. Sci. USA* **1999**, *96*, 14073–14078. [CrossRef]
66. The Global Posttranscriptional Regulator RsmA Modulates Production of Virulence Determinants and *N*-Acylhomoserine Lactones in *Pseudomonas aeruginosa*. *J. Bacteriol.* **2002**, *184*, 335. [CrossRef]
67. Luo, Z.W.; Cho, J.S.; Lee, S.Y. Microbial production of methyl anthranilate, a grape flavor compound. *Proc. Natl. Acad. Sci.* **2019**, *116*, 10749–10756. [CrossRef] [PubMed]
68. Miura, T.; Sánchez, R.; Castañeda, L.E.; Godoy, K.; Barbosa, O. Shared and unique features of bacterial communities in native forest and vineyard phyllosphere. *Ecol. Evol.* **2019**, *9*, 3295–3305. [CrossRef] [PubMed]
69. Martins, V.; López, R.; Teixeira, A.; Gerós, H. Combined omics expose microbial niches of fungi and bacteria correlating with wine volatile profiles in Douro wine region. *Lwt* **2024**, *193*, 115769. [CrossRef]

Disclaimer/Publisher's Note: The statements, opinions and data contained in all publications are solely those of the individual author(s) and contributor(s) and not of MDPI and/or the editor(s). MDPI and/or the editor(s) disclaim responsibility for any injury to people or property resulting from any ideas, methods, instructions or products referred to in the content.